Journal of
Nanoscience and Nanotechnology
Vol. 6, 2175–2181, 2006

Fabrication of Nanopores in a 100-nm Thick Si_3N_4 Membrane

Jae-Hyun Chung†, Xinqi Chen, Eric J. Zimney, and Rodney S. Ruoff*

Department of Mechanical Engineering, Northwestern University, Evanston, IL, 60208, USA

Textured alumina films have been used to fabricate nanoscale pores in Si_3N_4 membranes. A few nanometer-thick alumina layer was used as a masking material for nanopore fabrication, and the pattern was transferred into a 100-nm thick, 200 μm × 200 μm Si_3N_4 membrane by reactive ion etching (RIE). The nanopores were found to be concentrated in a ~150-μm diameter region at the center of the membrane.

Keywords: Nanopores, Reactive Ion Etching, Si_3N_4 Membrane, Alumina Film.

Interest in nanopore fabrication has grown in recent years. A few techniques have been developed for the fabrication of nanopores. Anodized aluminum is a nanoporous material that has been used, e.g., as a template for nanostructure synthesis,[1,2] and as a shadow mask in the patterning of nanodots over large surface areas (i.e., 1×1 cm^2).[3] A one-dimensional array of nanopores horizontally aligned with the substrate surface has also been fabricated by anodization of aluminum.[4] Polycarbonate membranes made by the track etch method[5] have pores with diameters as small as 10 nm. Such nanoporous membranes have been used as filter paper in the purification of single walled carbon nanotubes in suspension[6] and as a template in the synthesis of gold nanowires.[7] In applications where a small number of pores are required, electron beam lithography in combination with reactive ion etching (RIE)[8] as well as focused ion beam (FIB) micromachining[9] have been used to fabricate a small number of nanopores in a Si_3N_4 membrane.

The aluminum anodization process provides precise control over the diameter of nanopores, however it is challenging to fabricate pores in thin membranes (i.e., less than 100 nm thick). In addition, both FIB and RIE in combination with e-beam lithography are not currently able to readily fabricate large arrays of nanopores due to the serial scanning of the ion or electron beam. This paper presents a simple method to fabricate a random array of nanopores in a thin (~100 nm) Si_3N_4 membrane using an alumina layer, itself containing small pores, as a masking material. RIE was used to etch through the Si_3N_4 membrane so the pore pattern naturally present in the alumina film was transferred into the membrane.

A nanoporous membrane was fabricated on a silicon (Si) substrate whose size (*length* × *width* × *thickness*: 2.8 mm × 2.8 mm × 0.28 mm) was compatible with a standard transmission electron microscope (TEM) specimen holder; the fabricated nanopores could thereby be readily imaged in a TEM. The process used in the fabrication of the nanoporous Si_3N_4 membrane is as follows. First a 100-nm thick Si_3N_4 layer was deposited on a Si wafer (⟨100⟩, 1 Ω-cm resistivity, *p*-type, 0.28 mm thick; Polishing Corporation of America) using the low-pressure chemical vapor deposition (LPCVD) method. A square membrane was then defined on the Si_3N_4 layer by photolithography, and the pattern was transferred into the film by RIE (etch time: 1 min, plasma power: 100 Watts, process gasses: $CF_4 + O_2$; STS 340 RIE). KOH (45% by vol; J. T. Baker) was used to etch completely through the Si substrate forming a 100 nm thick, 200×200 μm^2 Si_3N_4 membrane. An aluminum layer was then deposited on the top surface of the Si_3N_4 membrane using electron-beam evaporation (Varian Electron Beam Evaporator) under vacuum (5×10^{-7} Torr). A quartz crystal monitor was used to detect the thickness of the aluminum layer and to control the deposition rate (~0.5 Å/sec). Four different thicknesses of aluminum were used as masking layers, namely 10.0, 6.0, 2.5, and 2.0 nm. The aluminum film was oxidized very quickly upon exposure to air converting it to alumina. Following the deposition of aluminum and exposure to air (ambient), the Si_3N_4 membrane was etched by RIE (etch time: 30, 40, 50, 60, or 70 sec., plasma power: 100 Watts, CF_4 and O_2 gases) forming nanopores in the Si_3N_4 membrane. As a final step, the alumina mask was removed by placing the Si substrate into Piranha solution ($H_2SO_4 + H_2O_2$) for ~5 minutes. Fifty-six Si_3N_4 membranes (array of 4×14 chips covering an area of 12×42 mm^2) were fabricated

*Author to whom correspondence should be addressed.
†Present address: Department of Mechanical Engineering, University of Washington, Seattle, WA, 98195, USA.

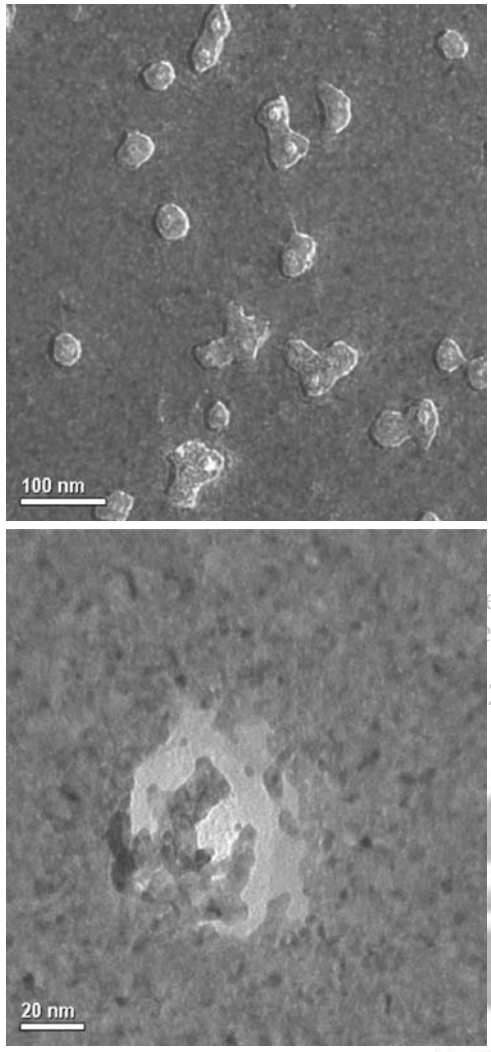

Fig. 1. TEM images of a Si_3N_4 membrane with a 2 nm thick alumina masking layer etched by RIE for 30 seconds. The alumina masking layer was removed prior to imaging. (a) An image of the nanoporous membrane and (b) magnified image of a single nanopore. The membrane was not completely etched through by the RIE and thus bowl shaped structures were achieved. The bowl diameter ranges from 50 to 55 nm.

in a single Si wafer to assess the yield of this process for nanopore fabrication.

For the samples with a 2.0 nm thick alumina masking layer, the Si_3N_4 membrane was etched for 30 seconds by RIE, followed by the removal of the masking layer in Piranha solution. The RIE etching time was selected because it is equal to the time required to completely remove an unmasked 100 nm thick Si_3N_4 film from a Si substrate. When imaged by a light microscope (Irvine Optical Ultrastation), the color of the membrane appeared uniform over the entire surface, identical to an un-etched Si_3N_4 membrane. A pitted structure was observed in the Si_3N_4 membrane by SEM (FEI Quanta ESEM). The samples were then imaged in a TEM (Hitachi HF-2000), which confirmed the formation of nanopores in the Si_3N_4 membrane [Fig. 1]; however, the pores were not etched completely through the membrane. Thus "nano-bowls" rather then nanopores were created in the Si_3N_4 membrane.

An identical Si_3N_4 membrane with a 2.0 nm thick alumina masking layer was etched for 40 seconds in the RIE under identical conditions. Following etching the membrane was imaged in a light microscope where it was found that a roughly circular area ($\sim$150 μm in diameter) in the center of the square membrane appeared darker in color [Fig. 2(a)]. The darkening of the Si_3N_4 membrane is possibly due to a change in the photonic band gap of Si_3N_4 in the presence of the nanopores.[10, 11] Following the removal of the alumina masking layer in Piranha solution, the Si_3N_4 membrane was imaged by SEM (LEO Gemini 1525), which showed that a densely packed array of nanopores was created in the center of the Si_3N_4 membrane [Fig. 2(b)]. Imaging in the TEM indicated that the pores had now been etched completely through the membrane. SEM imaging also indicated that the density of the nanopores decreased with distance from the center of the membrane [Figs. 2(c) and (d)] with only a few pores created near the edge of the membrane. The diameter of the nanopores was quite uniform over the entire Si_3N_4 membrane with diameters ranging from 50 to 55 nm as measured in the SEM [Fig. 2].

Figure 3 compares the normalized nanopore density to the normalized color contrast (i.e., the pixel color number [*dark green*: 255 and *bright yellow*: 0] divided by 255, the maximum color number) of an image of the Si_3N_4 membrane taken with a light microscope (Irvine Optical Ultrastation with a ultra-violet (UV) filter). The color contrast observed in the light microscope image is conceivably caused by a change in the optical band gap of the Si_3N_4 membrane, which is related to the density of nanopores in the membrane. The dark color (i.e., lower contrast) marks the region of high pore density, which was verified in the SEM [Fig. 2].

Further etching of a porous membrane (i.e., a membrane with pores that have already been etched through the membrane) resulted in the collapse of the membrane. Figure 4 shows SEM images of a membrane following 60-seconds of etching in the RIE. The center area (140×140 μm^2) of the membrane has been completely removed, and a mesh structure was formed near the edge. Therefore optimizing the etching time is critical for achieving pore formation without damaging the membrane.

A 2.5 nm thick alumina masking layer with an RIE etching time of 50 seconds yielded nanopores in another set of 100 nm thick, 200 μm $\times$ 200 μm Si_3N_4 membranes. Again, the central region of the membrane (150 μm in diameter) appeared darker in color when imaged by a light microscope. The center of the membrane was broken using the tip of a tungsten probe (3.5 μm tip diameter, Signatone SE-20T) to allow for cross-sectional imaging in the SEM. The alumina mask was left intact on the Si_3N_4 membrane to assess the relationship between the pores in the alumina layer and the nanopores in the membrane [Fig. 5].

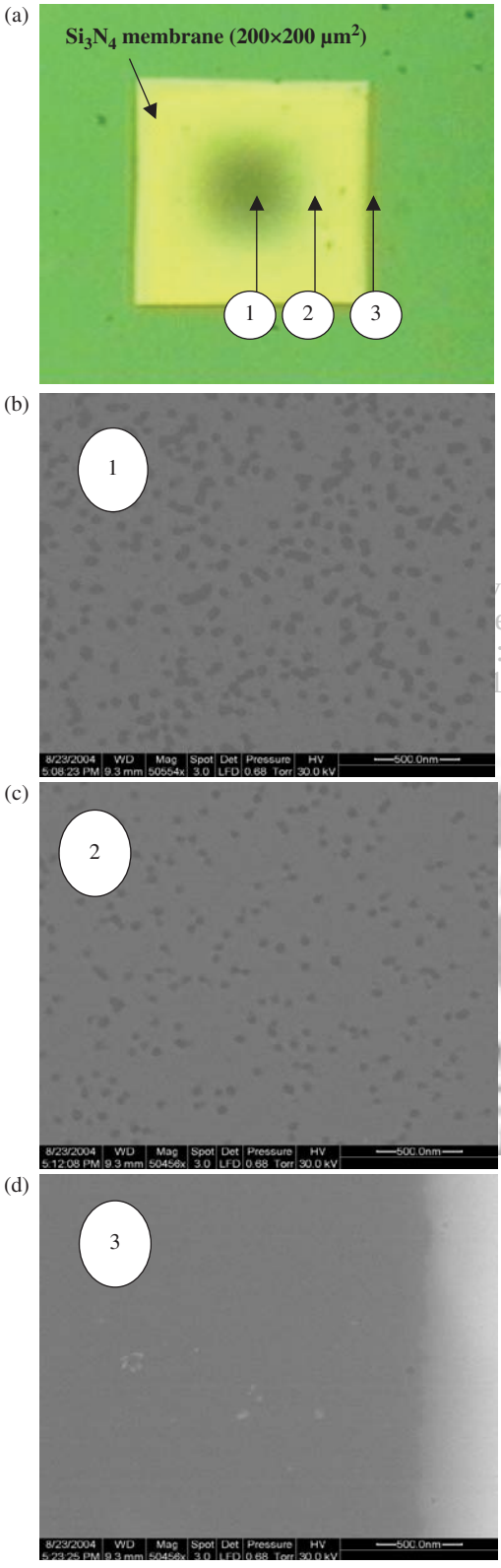

Fig. 2. Images of a nanoporous Si_3N_4 membrane formed with a 2 nm thick alumina masking layer etched by RIE for 40 seconds. The alumina masking layer was removed prior to imaging. (a) Light microscope image of the Si_3N_4 membrane. (b)–(d) SEM images of the membrane taken (b) 0 μm (pore density: 50.4/μm^2), (c) 50 μm (pore density: 29.6/μm^2), and (d) 100 μm (pore density: 0.8/μm^2) from the center of the membrane.

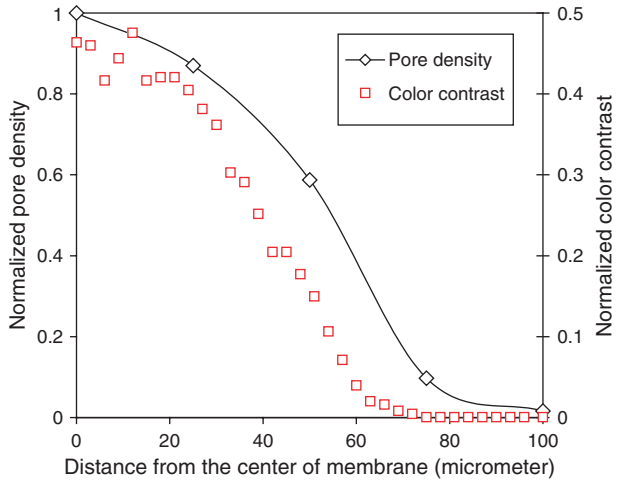

Fig. 3. A plot of the normalized color contrast of a light microscope image of a nanoporous membrane and normalized nanopore density in the Si_3N_4 membrane (nanopore density: 1=50.4/μm^2) verses distance from the center of the membrane. The change in color contrast of the light microscope image is a measure of the density of nanopores (higher the normalized contrast the higher the pore density) in the Si_3N_4 membrane.

Figure 5(b) is a SEM image of the structure of the alumina mask and the nanoporous membrane where the white region is the alumina masking layer, the dark grey region is Si_3N_4 that has been exposed by etching of the alumina mask, and the black dots are nanopores created in the membrane. Figure 5(b) proves that the alumina layer functioned as a mask during the RIE etching process. The diameter of the nanopores ranged from 17 to 30 nm suggesting that the thickness of the alumina masking layer can affect the diameter of the nanopores; however, more tests are needed to ascertain any relationship between alumina thickness and nanopore diameter.

The same broken Si_3N_4 membrane was also imaged in the TEM. Figure 6 is a TEM image of a nanopore in a broken section of the Si_3N_4 membrane; the RIE process time (50 sec) yielded nanopores with constant cross sections in the Si_3N_4 membrane. The apparent wall thickness of the nanopore shown in Figure 6 is 10 nm. Since the actual thickness of the Si_3N_4 membrane was 100 nm, the tilt angle is ~5.7°. Accounting for this tilt angle, the diameter of the nanopore in Figure 6 was ~18 nm. Several nanopores were imaged in the TEM; all had a constant cross section and a roughly circular shape with a diameter close to ~20 nm.

For the thicker alumina films (10.0 and 6.0 nm), the Si_3N_4 membrane was etched by RIE for 60 seconds. The alumina layer was then removed in Piranha solution. SEM imaging showed that a porous structure was not formed in the Si_3N_4 membrane.

The key step in the fabrication process presented in this paper is the deposition of the alumina masking layer. When the substrate is initially exposed to the incident aluminum vapor, it is expected that the aluminum atoms

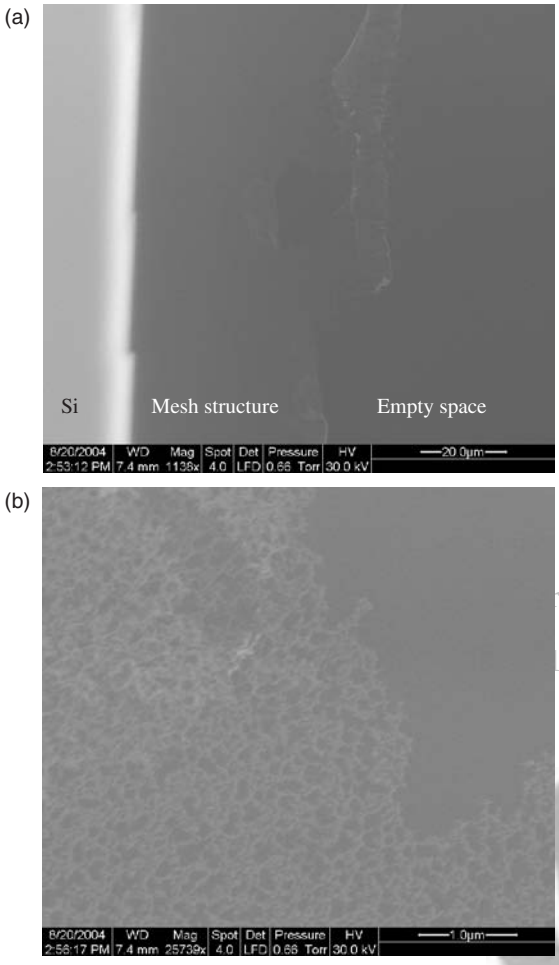

Fig. 4. SEM images of an over etched Si_3N_4 membrane (alumina masking layer thickness: 2 nm, RIE etching time: 60 seconds). (a) One edge of a membrane. The center part of the membrane was completely removed and a mesh structure is left near the edge. (b) A magnified view; mesh formed near the edge of the Si_3N_4 membrane.

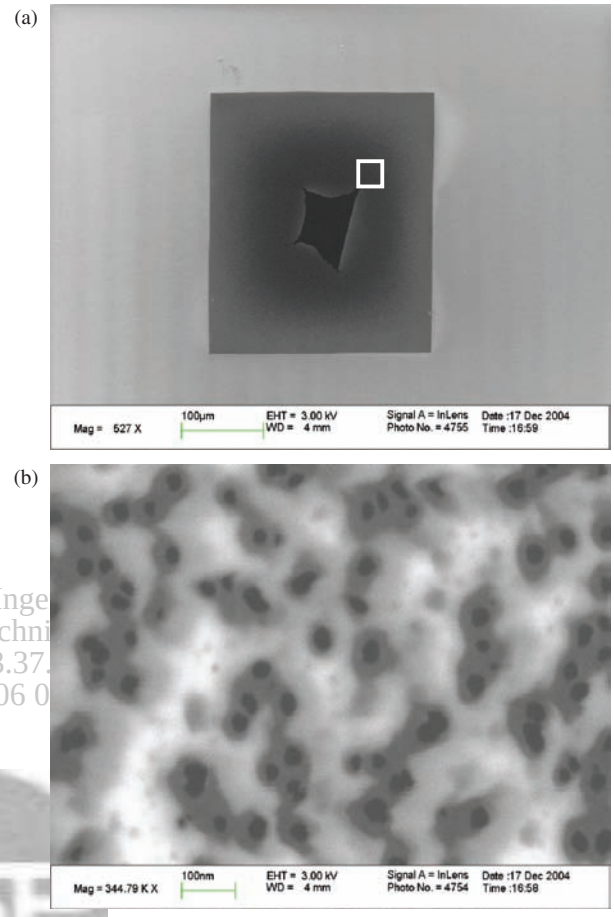

Fig. 5. SEM images of a Si_3N_4 membrane with a 2.5 nm-thick alumina masking layer etched by RIE for 50 seconds. The masking layer was not removed prior to imaging. (a) SEM image of the Si_3N_4 membrane that was intentionally broken for easier imaging. (b) Image of the Si_3N_4 membrane taken in the area indicated in (a). The diameter of the nanopores ranges from 17 to 30 nm.

condense and adhere to the substrate surface forming a uniform distribution of metal clusters or islands[12]. This is often referred to as the nucleation stage; as deposition continues, the metal islands merge and coalesce partially covering the substrate surface.[12] As more metal material is deposited on the surface, all available voids are ultimately filled, forming a continuous metal film. The alumina masking layer used in this study was only a few nanometers thick as measured by a quartz crystal monitor. At such a small thickness it is likely that the metal clusters on the substrate surface had begun to coalesce and form networks. The voids left by the coalescence of metal islands form the textured film pattern that was transferred by RIE into the Si_3N_4 membrane.

The chemical composition of the masking layer was investigated by X-ray photoelectron spectroscopy (XPS; Omicron ESCA probe equipped with an EA125 energy analyzer). The analysis was performed on a 2 nm-thick alumina layer. A 100 nm thick Si_3N_4 film was deposited on a Si (100) substrate using LPCVD, and then a 2.0 nm thick aluminum layer was deposited onto the Si_3N_4 using electron-beam evaporation. Photoemission was stimulated by a monochromated Al KR radiation (1486.6 eV) with an operating power of 300 W. The analyzer was operated in the constant analyzer energy (CAE) mode at a pass energy of 60 eV of the electrons through the center line of the hemispheric analyzer. Binding energies were referenced to the C 1s binding energy set at 285.0 eV. (A survey scan for binding energies, not shown, was performed from 0 to 1200 eV).

Figure 7 shows the XPS spectrum for binding energies from 0 to 700 eV. Oxygen, aluminum, silicon, nitrogen, and carbon peaks were detected in this range. Quantitative analysis revealed that the surface of the sample contained ~32.7 at.% Al, ~56.6 at.% O, ~5.9 at.% Si, ~2.3 at.% N, and ~2.5 at.% C. The small amount of carbon probably was due to surface contamination because the sample was exposed to air for several days. From the peak positions (531.9 eV for O 1s, 74.4 eV for Al 2p, 101.4 eV for Si 2p, 397.4 eV for N 1s), silicon nitride and amorphous

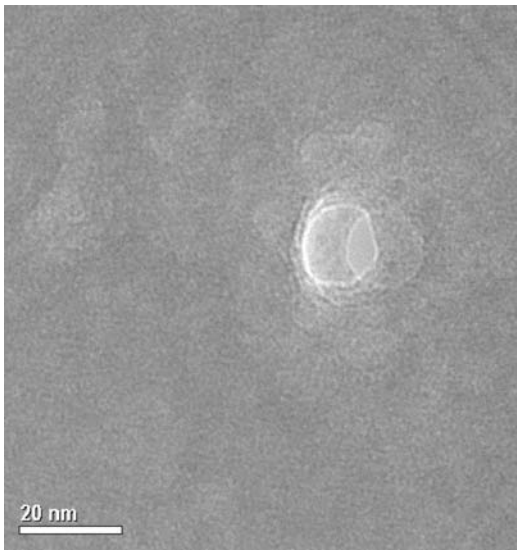

Fig. 6. TEM image of a nanopore in the same Si_3N_4 membrane shown in Figure 5. This nanopore was located in a broken portion of the membrane. Based on the apparent wall thickness of the nanopore (~10 nm) and the actual thickness of the Si_3N_4 membrane (~100 nm) the tilt angle between the pore axis and the beam axis is calculated to be ~5.7°. Based on this analysis the diameter of the nanopore is ~18 nm.

aluminum oxide are present. Aluminum oxide has been formed while the sample was exposed to air. The silicon and nitrogen likely are from exposed silicon nitride film because the 2.0 nm thick aluminum film may not fully cover the silicon nitride surface. The extra oxygen (taking account of the O:Al ratio for Al_2O_3) might be due to Si–O bond formed on the silicon nitride surface and/or surface contamination.

In an effort to determine why the nanopores are concentrated in the center of the Si_3N_4 membrane, the 2.0 and 2.5 nm thick alumina masking layers were surveyed by atomic force microscopy (AFM: JEOL 5200) prior to etching in the RIE. AFM images showed that the distribution of nanopores in the alumina film was essentially uniform over the entire Si_3N_4 film including the film on Si substrate for both 2.0 and 2.5 nm alumina layer. The non-uniform distribution of pores in the Si_3N_4 membrane must therefore arise from the RIE process. Further characterization of the pristine alumina mask in the SEM and TEM was performed but was unsuccessful. It was challenging to get high resolution images of the masking layer in the SEM due to charging of the non-conductive alumina film and Si_3N_4 membrane. Also the alumina layer could not be readily imaged in the TEM due to the thickness (100 nm) of the Si_3N_4 membrane.

In Figure 8 are SEM images of the 2.5 nm thick alumina layer on a Si_3N_4 membrane following 50 seconds of etching in the RIE. The alumina masking layer (white color in Fig. 8) in the center of the membrane was etched more than that near the edge of the membrane suggesting the etching rate is higher in the center of the membrane then near the edges. This effect was also observed in the etching of Si_3N_4 membranes without the alumina masking layer. Two different sized Si_3N_4 membranes (1000×1000 μm^2 and 30×30 μm^2) were fabricated using the same process

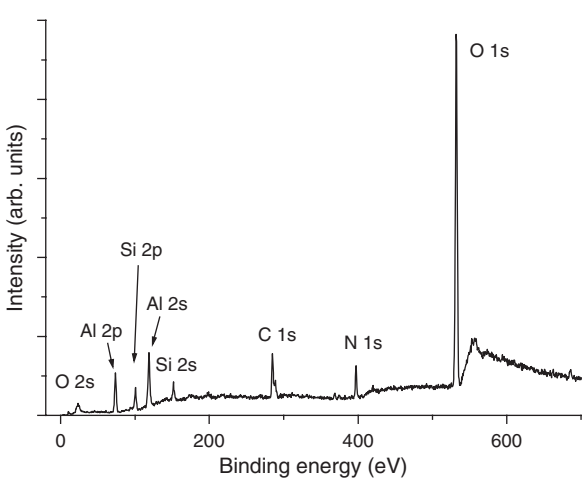

Fig. 7. XPS survey scan results; the peaks of O 1s and 2s, Al 2s and 2p, Si 2s and 2p, N 1s, and C 1s were observed.

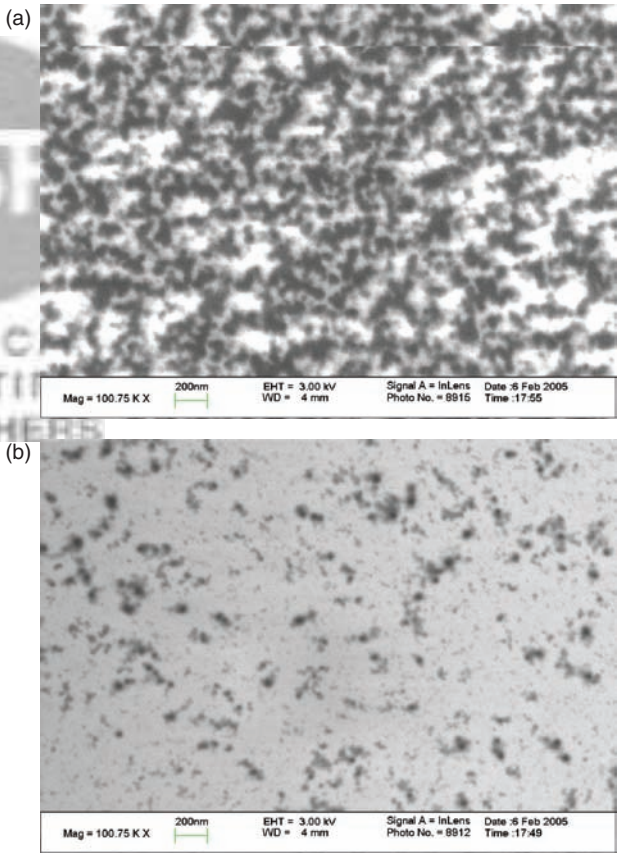

Fig. 8. SEM images of an alumina masking layer on a Si_3N_4 membrane etched by RIE for 50 seconds. (a) SEM image of the highly porous alumina layer in the center of the membrane (white area shows alumina layer). (b) SEM image taken near the edge of the membrane showing a less porous alumina layer. These images show that etching of the masking layer was faster in the center of the membrane than near the edge.

Table I. Yield: Success (✓) and failure (×) (yield = 66%[a]).

	1	2	3	4	5	6	7	8	9	10	11	12	13	14
1	✓	✓	✓	✓	✓	✓	×	✓	✓	✓	×	×	×	×
2	✓	✓	✓	✓	✓	✓	✓	✓	✓	✓	×	×	×	×
3	✓	✓	✓	✓	✓	✓	✓	✓	×	×	✓	×	×	×
4	✓	✓	✓	✓	✓	✓	✓	✓	×	✓	×	×	×	×

[a]note that yield for "left region" could be considered as 27/28, or 31/32.

outlined above and then etched by RIE for 10 sec. Note that 30 seconds of RIE is needed in order to remove a 100 nm thick Si_3N_4 film (not suspended) from the Si substrate. Following the RIE, the center of the 1000×1000 μm^2 membrane was completely removed forming a large hole. A hole was, however, not found in the 30×30 μm^2 membrane. We speculate that the etching in the center of the membrane may be more aggressive, because the membrane is more compliant in the center than near the edge. The energetic ions exert pressure on the membrane causing an increase in the stiffness near the edge of the membrane, which leads to a decrease in the etching rate. Similarly, the smaller membrane (30×30 μm^2), which has a higher stiffness, had a slower etching rate. The mechanism that leads to the distribution of etching rates across the membrane has not been clearly determined and could be the focus of further work.

During the RIE plasma process used to etch Si_3N_4, CF_4 molecules have been reported to dissociate to yield cations such as CF_3^+, COF_2^+, CO_2^+, O_2^+, O^+, F^+, and F_2^+ [12–14]; electrons and anions such as F^- are likely also present. Physicochemical etching of the Si_3N_4 film is realized by some or all of these reactive and charged species, and in particular the cations and any neutral species are expected to play a role, because the Si chip array with the Si_3N_4 film was mounted on the cathode in the plasma etcher.

Counting the number of membranes with a darkened region in the center provided a quick measure for the yield of the fabrication process. Imaging with a light microscope indicated that nanopores using a 2 nm thick alumina layer were successfully created in 37 out of the 56 membranes on a single Si substrate [Table I]. Thus the current fabrication process has a moderate yield of 66%; however we note that the success rate was much higher for those membranes in the "left region" of the array of chips. This yield was consistent for several Si wafers with either the 2.0 or 2.5 nm thick alumina masking layer. The uneven etching of the Si wafer was ascribed to the RIE system used in this experiment. It was observed that the etching rate was higher in the center of the RIE. To improve the yield, the Si wafer may be moved with respect to the plasma so that each group of chips has a similar etching rate. This was not possible with the RIE system used in this study. Another potential method of improving the process yield is to identify those chips in which pores were not created using optical microscopy and etch them for an additional amount of time in the RIE.

In conclusion, 100-nm thick Si_3N_4 membranes with a random array of nanopores were successfully fabricated using a thin alumina layer as a masking material. The alumina layer is itself nanoporous, and the pore pattern was transferred into the underlying Si_3N_4 membrane using RIE etching. The nanopores were concentrated in the center of each square membrane. Compared to other methods, this method is a relatively straightforward way to create nanopores in a thin Si_3N_4 (thus, dielectric) membrane. Potential applications of the nanoporous membrane include as a TEM substrate, as a component in a biosensor, or as filter paper, among other potential applications.

Acknowledgments: We appreciate comments from R. Krchnavek, and support from the Naval Research Laboratory (grant No. N00173-04-2-C003), and the NSF (CMS-0304506; NIRT: Synthesis, Characterization, and Modeling of Aligned Nanotube Arrays for Nanoscale Devices, Ken Chong program manager). All TEM and SEM work was performed in the Electron Probe Instrumentation Center (EPIC) facility of the NUANCE Center at Northwestern University. The NUANCE Center is supported by NSF-NSEC, NSF-MRSEC, Keck Foundation, the State of Illinois, and Northwestern University.

References and Notes

1. P. L. Chen, J. K. Chang, C. T. Kuo, and F. M. Pan, *Appl. Phys. Lett.* 86, 123111 (**2005**).
2. T. T. Xu, F. T. Fisher, L. C. Brinson, and R. S. Ruoff, *Nano Lett.* 3, 1135 (**2003**).
3. K. Liu, J. Nogues, C. Leighton, H. Masuda, K. Nishio, I. V. Roshchin, and I. K. Schuller, *Appl. Phys. Lett.* 81, 4434 (**2002**).
4. H. Zhang, Z. Chen, T. Li, and K. Saito, *J. Nanosci. Nanotechnol.* 5, 1745 (**2005**).
5. E. Ferain and R. Legras, *Nucl. Instr. and Meth. in Phys. Res. B* 208, 115 (**2003**).
6. J. Liu, A. G. Rinzler, H. J. Dai, J. H. Hafner, R. K. Bradley, P. J. Boul, A. Lu, T. Iverson, K. Shelimov, C. B. Huffman, F. Rodriguez-Macias, Y. S. Shon, T. R. Lee, D. T. Colbert, and R. E. Smalley, *Science* 280, 1253 (**1998**).
7. M. Wirtz and C. R. Martin, *Adv. Mater.* 15, 455 (**2003**).
8. K. S. Ralls, R. A. Buhrman, and R. C. Tiberio, *Appl. Phys. Lett.* 55, 2459 (**1989**).
9. J. Li , D. Stein, C. McMullan, D. Branton, M. J. Aziz, and J. A. Golovchenko, *Nature* 412, 166 (**2001**).
10. M. D. B. Charlton and G. J. Parker, *J. Micromech. MIcroeng.* 8, 172 (**1998**).

11. M. C. Netti, M. D. B. Charlton, and J. J. Baumberg, *Appl. Phys. Lett.* 76, 991 **(2000)**.
12. M. Ohring, *Materials Science of Thin Films*, Academic Press, San Diego **(2002)**.
13. M. Madou, *Fundamentals of Microfabrication*, CRC press, New York **(2002)**.
14. I. Ishikawa, S. Sasaki, K. Nagaseki, Y. Saito, and S. Suganomata, *Jpn. J. Appl. Phys.* 36, 4648 **(1997)**.

Received: 13 January 2006. Revised/Accepted: 30 April 2006.